

RADIATION-INDUCED ALTERATIONS IN THE ELECTRICAL CHARACTERISTICS OF PEDOT:PSS/CNT NANOCOMPOSITES

I. Zhydenko^{1,2}, H. Klym^{2,3}

¹*Lviv State University of Life Safety*
35 Kleparivska St. UA-79007, Lviv, Ukraine
zhidenkoillya@gmail.com, illia.v.zhydenko@lpnu.ua

²*Specialized Computer Systems Department,*
Lviv Polytechnic National University,
12 Bandery St., UA-79013, Lviv, Ukraine
halyna.i.klym@lpnu.ua, klymha@yahoo.com

³*Radioelectronic and Computer Systems Department,*
Ivan Franko National University of Lviv,
50 Drahomanova St., UA-79005 Lviv, Ukraine
halyna.klym@lnu.edu.ua

The impact of β - and γ -radiation on the electrical characteristics of nanocomposites derived from the combination of poly(3,4-ethylenedioxythiophene)-poly(styrenesulfonate) and multi-walled carbon nanotubes was investigated. The results demonstrate that the radiation dosage induces alterations in the electrical properties of these nanocomposites. An increase in the quantity of conductive nanotubes within the polymer matrix is associated with a reduction in electrical resistance and an enhancement in their responsiveness to radiation. This study establishes that radiation-induced transformations are observed in both the polymer matrix and the nanotubes.

Key words: nanocomposite, nanotube, radiation, polymer matrix, electrical properties, computer simulation.

Introduction. Nanocomposites, characterized by the incorporation of nanoscale filler materials into a dielectric (polymer) matrix, have long been recognized for their remarkable mechanical and electrical attributes [1,2]. These extraordinary properties have opened up exciting possibilities in various fields, from sensor technologies to radiation shielding materials.

The creation of mechanically stable nanosystems with specific geometries through the aggregation of carbon nanotubes has led to the development of composites with enhanced characteristics [3,4]. These advanced materials find applications in sensors and as effective radiation shielding materials. Notably, epoxy resins, when reinforced with nanofillers, and polymers infused with carbon nanotubes, have emerged as highly promising candidates in this regard [5-7].

The potential for macroaggregation and condensation of nanotubes within mechanically stable systems possessing specific geometries has significantly expanded the scope for the creation of sound-absorbing and radiation-shielding materials with diverse applications [8-11]. For instance, epoxy resins reinforced with various nanostructures have been the focus of intensive research over the past decade. Additionally, nanotubes integrated into conductive polymers with conjugated chains have garnered substantial interest.

These systems, such as epoxy resins with reinforced nanostructures, have been the subject of extensive investigations in recent years, as have polymers with varying concentrations of nanotubes within electrically conductive matrices with interconnected chains.

The distinctive electrical properties inherent to polymers and their associated nanocomposites render them well-suited for deployment in detecting chemical or biological agents, particularly as sensitive components in ionizing radiation detectors [12,13]. The technology for designing radiation nanocomposite sensors is relatively cost-effective and straightforward. To optimize the performance of these sensor elements, it is imperative to explore the impact of irradiation dose on the electrical conductivity of nanocomposites. This necessitates a comprehensive study of key parameters, such as nanofiller concentration, among others.

The primary objective of this study is to employ computer simulations to investigate the effects of β - and γ -radiation on the electrical properties of PEDOT:PSS/CNT nanocomposites. By shedding light on how these radiation types influence the conductive characteristics of the composite material, we aim to contribute valuable insights to the development of effective radiation sensors.

Experimental. In our research aimed at studying the radiation-resistant properties of PEDOT:PSS/CNTs composite structures, we undertook a series of meticulously designed experimental procedures. The starting materials, PEDOT:PSS polymer (1.5% aqueous suspension), and multiwall nanotubes (CNTs), were sourced from Sigma-Aldrich Co. in the United States.

The multiwall nanotubes, characterized by an average length of 30 μm and dimensions ranging from 8 to 15 nm, were introduced into the polymer matrix with the intention of achieving homogenous dispersion. To facilitate this, an ultrasonic treatment was carried out in a solution of nitric and sulfuric acids at a 3:1 ratio. The CNTs were carefully dosed at a concentration of 0.5 mg per 1 ml of the mixture. Following this step, the CNTs underwent multiple rinses with distilled water to eliminate any residual acids. Subsequently, the CNTs were combined with the PEDOT:PSS solution and subjected to ultrasonic treatment for an extended period of 8 hours. The resulting composition was then deposited onto a glass substrate and allowed to dry for a period of 48 hours at room temperature. This meticulous process yielded a monolithic PEDOT:PSS/CNTs film, notable for its thickness exceeding 20 μm .

In our experiments, we employed nanocomposite compositions with varying nanotube concentrations, specifically around 5%, 7.5%, and 10%. For comparative purposes and as a reference point in our investigations, we also included PEDOT:PSS films devoid of any nanotube additives [14,15].

To gain insight into the nanostructures formed within the composite films, we employed a high-resolution scanning electron microscope (SEM). Through careful selection of the electron mode and energy parameters, we were able to capture clear and detailed images. Our SEM analyses revealed a characteristic feature of nanocomposites: the aggregation of nanotubes

within the polymer matrix. This observation is vividly depicted in Fig. 1, which illustrates typical clusters of multiwall nanotubes within the composite structure at varying nanofiller concentrations.

To comprehensively assess the electrical properties of these hybrid nanocomposites, we established electrical contacts on the sample surfaces. The distance between these contacts was maintained at approximately 5 mm, while the thickness of the samples exceeded 0.5 μm . This setup was instrumental in conducting our investigations into the conductivity and electrical characteristics of the materials.



Fig. 1. SEM image of investigated PEDOT:PSS/CNT nanocomposites.

To assess the electrical properties of our samples, we conducted measurements at room temperature across a frequency range spanning from 25 Hz to 1 MHz. The test signal amplitude was maintained at 25 mV. Two distinct instruments, namely the RLC meter E7-20 and the impedance analyzer Keysight E4990A, were employed for these measurements, each offering unique capabilities.

The Keysight E4990A impedance analyzer excels in measuring the impedance modulus, spanning an extensive range from 0.1 Ohm to 1 GOhm. Remarkably, the error associated with these measurements does not exceed 1% of the absolute value. This instrument proved invaluable in our investigations.

On the other hand, the RLC meter E7-20 extends its reach in measuring the impedance modulus from 10 Ohm to 10 MOhm. While this range is slightly more constrained than the Keysight analyzer, it still provides a comprehensive assessment. The error in these measurements is modest, not exceeding 3% of the absolute value. Moreover, the RLC meter E7-20 boasts the capability to measure phase shifts with an accuracy of 1 degree, specifically at operating frequencies spanning from several hundreds of Hz to 1 MHz. This instrument offers an additional advantage - the ability to record temperature-dependent dielectric losses, active,

and reactive components of electrical conductivity at a fixed frequency. To elevate the precision of our measurements, we introduced automation elements into the fundamental measurement circuits related to electrical conductivity and dielectric functions.

For precise control and regulation of temperature, we employed a computer-based system, ensuring heating and cooling processes adhered to a linear law, maintaining temperature control with an accuracy not less than 1 K. In the case of the RLC meter, measurements were conducted in an automatic mode, enhancing efficiency and reducing potential human error.

During the measurements, the test specimens were accommodated within a two-electrode cell featuring non-blocking electrodes. These electrodes were meticulously formed on opposite faces of the test specimens. The establishment of electrical contacts for the preparation of experimental samples involved the use of copper conductors and conductive adhesive, ensuring reliable and consistent contact points.

In our investigation into the impact of ionizing β - and γ -radiation on PEDOT:PSS/CNT nanocomposites, we employed the ^{226}Na isotope with an activity level of 0.1 mCi. The decay of the ^{226}Na isotope, with a 3.28% probability, emitted γ -rays with an energy of approximately 0.19 MeV. Similarly, the average energy associated with β -radiation was approximately 0.17 MeV. To maintain a consistent experimental setup, the samples were positioned at a distance of 0.6 meters from the radiation source. This distance rendered it unnecessary to account for α -particles, which are typically adsorbed within a few centimeters of air travel. The dose of radiation administered was estimated based on the duration of exposure [15].

Results and discussion. Fig. 2 illustrates the electrical resistance characteristics of PEDOT:PSS samples, without the inclusion of nanotubes, as a function of radiation dose and frequency. Notably, the response of these samples to radiation exposure is particularly intriguing.

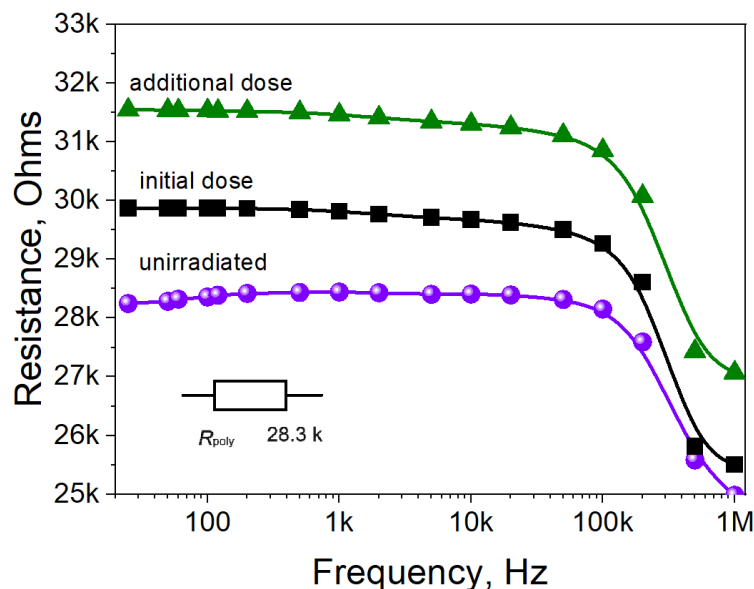


Fig. 2. Variation in electrical resistance of pure PEDOT:PSS composite with frequency at different radiation doses

Initially, for the non-irradiated sample, we observed an electrical resistance exceeding 28 kOhm within the low-frequency range, spanning from DC to 100 kHz. This resistance exhibited a decreasing trend, ultimately stabilizing at 25 kOhm as the frequency increased to 1 MHz. However, after subjecting the sample to a 30-minute irradiation period, a significant shift in electrical resistance became evident. Specifically, the resistance in the low-frequency range surged to over 2 kOhm, marking a notable increase in resistance. Astonishingly, this effect was magnified when an additional 30 minutes of irradiation was applied. Given that the conductivity of PEDOT:PSS composites remains frequency-independent below 100 kHz, we can effectively model the behavior of the measuring system as a simple R_{poly} resistance.

In Fig. 3, we delve into the electrical resistance versus frequency profiles for PEDOT:PSS/CNT nanocomposites. This figure presents an intriguing contrast compared to the non-nanotube-containing samples.

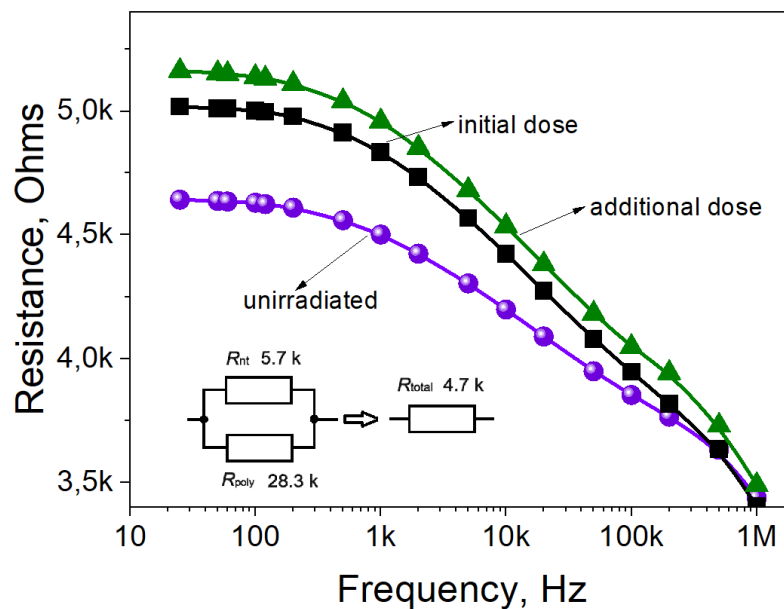


Fig. 3. Electrical resistance dependence of PEDOT:PSS/CNT nanocomposite with frequency at varied radiation levels

The most conspicuous observation is the remarkable reduction in low-frequency resistance, with values reaching as low as 4.7 kOhm for the non-irradiated nanocomposite samples. This marked reduction in resistance highlights the influence of the nanotubes on the electrical properties of the composite material and opens up intriguing possibilities for various applications. Further analysis of these effects and their implications is essential to fully understand the behavior of these nanocomposite materials in response to radiation exposure.

As is widely known, the conductive properties exhibited by polymers bear a striking resemblance to those of inorganic semiconductors. In this context, it is plausible to attribute the decline in electrical resistance to the metallic properties inherent in carbon nanotubes. Under this assumption, we can conceptualize that the nanotubes form a parallel pathway for electrical conduction alongside the pathway already established by the polymer structures. Consequently,

the overall low-frequency resistance of PEDOT:PSS/CNT nanocomposites can be effectively modeled as the parallel connection of two resistances: R_{poly} and R_{nt} , representative of the polymer matrix and nanotubes, respectively. By comparing the experimentally measured low-frequency resistance of 4.7 kOhm to the calculated value resulting from the combination of these parallel resistors, we deduced that the nanotube resistance, R_{nt} , is approximately 5.7 kOhm.

As illustrated in Fig. 4, an increase in the proportion of nanotubes incorporated into the polymer matrix correlates with a notable reduction in the electrical resistance of the resulting nanocomposites. This trend underscores the significance of nanotubes in influencing the electrical properties of the composite materials, a feature that holds promise for various practical applications.

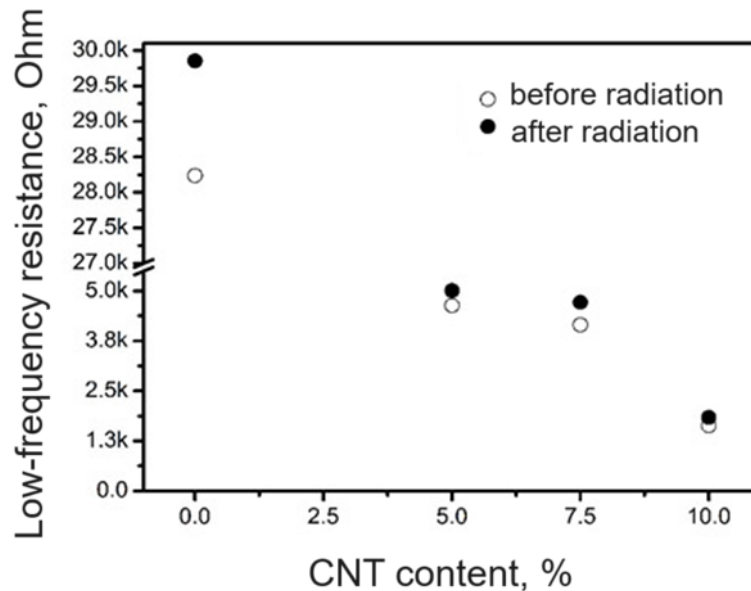


Fig. 4. Influence of nanotube content on low-frequency resistance before and after absorption of γ -quanta

To validate our experimental findings, we conducted numerical simulations. In these simulations, the nanotube-filled polymer matrix was modeled as a three-dimensional parallelepiped, featuring electrodes positioned on opposite sides and an assortment of randomly distributed open nanotubes with cylindrical geometry. The search algorithm, primarily founded on graph theory, dictated the dominant pathways within this simulated nanocomposite. These simulations were computationally intensive and required substantial computational resources.

The outcomes of our simulations provided insights into the spatial distribution of nanotubes within the volume and identified the dominant conduction pathways, as depicted in Fig. 5.

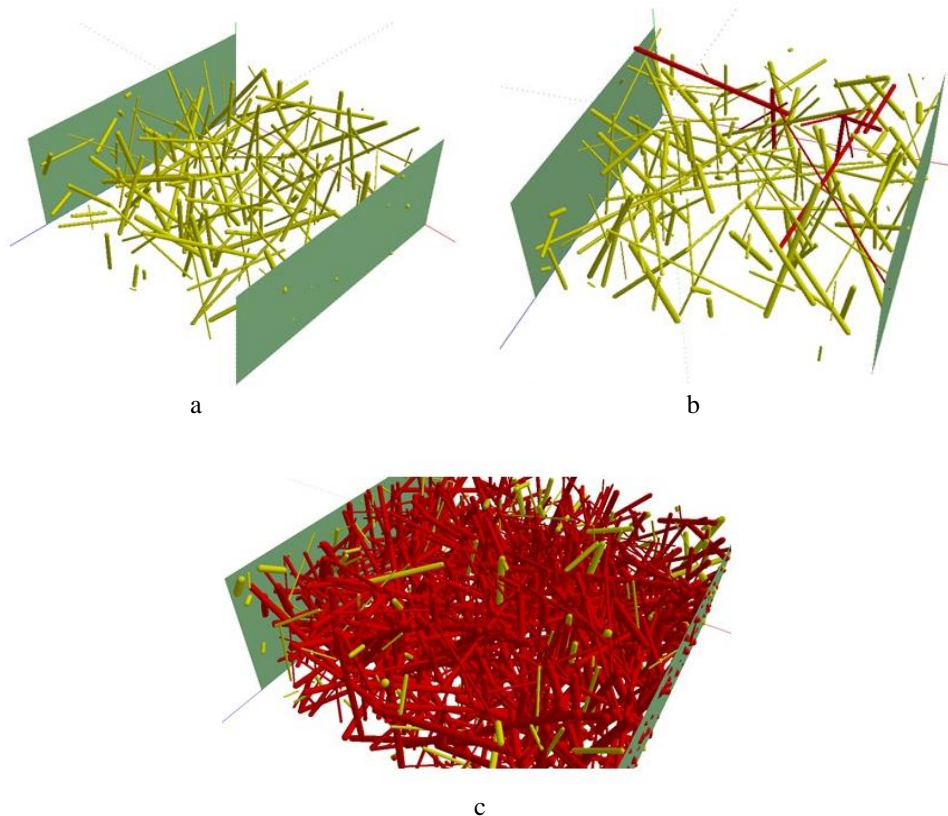


Fig. 5. Computational modeling of nanotube distribution in polymer matrix: a - absence of conductive path; b - single leading path; c - multiple leading paths.

Interestingly, the simulated percolation threshold, which denotes the minimum nanotube concentration required to achieve electrical conductivity, was found to be approximately 1%. This value suggests that a relatively low nanotube concentration is needed to form conductive paths within the nanocomposite, a finding that contrasts with the experimentally determined percolation threshold. Discrepancies between these results could be attributed to various factors, such as limitations inherent in the model (e.g., limited elements in the system compared to the number of nanotubes in experimental samples) or differences in the dispersion conditions of nanotubes during sample preparation.

Fig. 2 and Fig. 3 provide insights into the response of PEDOT:PSS/CNT nanocomposites to β - and γ -radiation emitted by a ^{226}Ra source. These radiations induce a notable increase in electrical resistance within the nanocomposite, a phenomenon attributed to simultaneous changes in both R_{nt} and R_{poly} . If we consider that only R_{poly} is exposed to radiation, following the initial radiation dose, the total resistance of the nanocomposite remains constant at 5.7 kOhm (as previously described). This constant R_{nt} is in parallel with the initial R_{poly} value of 30 kOhm, as indicated by the blue curve in Fig. 2.

Consequently, our calculated total resistance of 4.8 kOhm, as opposed to the experimental value of 5 kOhm, as indicated in Figure 3, suggests that our initial assumption—that only Rpoly is affected by radiation—is not entirely accurate. It becomes apparent that radiation-induced changes impact both Rnt and Rpoly parameters within the nanocomposite.

One plausible explanation for the increase in Rpoly lies in the context of radiation-triggered parallel degradation processes and alterations in polymer bonding. The absorption of ionizing radiation can result in the breakage of polymer chains, causing charge transfer through π -electron conjugations. This, in turn, leads to enhanced electrical conductivity within the hybrid system. Conversely, when incomplete bonds with uncompensated valence electrons are formed, it can result in chain blocking and the stimulation of polymer "crosslinking." These transformations are inherently irreversible, and the extent of the changes is contingent upon the radiation dose and the specific structure of the polymer.

In essence, ionizing radiation exerts a multifaceted influence on the electrical properties of the nanocomposite, involving changes in both the nanotube resistance (Rnt) and the polymer resistance (Rpoly). Understanding these intricate interactions is pivotal for a comprehensive assessment of the radiation-induced effects on the material's behavior. Further investigation is essential to elucidate the exact mechanisms at play and to harness this knowledge for practical applications in radiation-sensitive materials.

Conclusion. We embarked on the creation of nanocomposites based on poly(3,4-ethylenedioxythiophene)-poly(styrene-sulfonate) (PEDOT:PSS), and seamlessly integrated multi-walled carbon nanotubes (CNTs) into the matrix. Our research has conclusively demonstrated that these fabricated nanocomposites exhibit sensitivity to varying doses of β - and γ -radiation.

The inclusion of conductive carbon nanotubes in the polymer matrix plays a pivotal role in this sensitivity. Notably, the incorporation of CNTs serves a dual purpose: it reduces the electrical resistance within the systems while simultaneously enhancing their responsiveness to radiation-induced changes. These alterations in the electrical properties are not exclusive to the polymer matrix alone; rather, they also manifest within the nanotubes themselves.

This intriguing discovery opens up a realm of possibilities for practical applications. The resultant structures can serve as highly effective components in radiation sensors, facilitating the precise detection of ionizing radiation. Furthermore, they can be employed as protective coatings for electronic equipment, offering a shield against the potentially harmful effects of radiation exposure. Thus, our research underscores the versatility and utility of these PEDOT:PSS/CNT nanocomposites in the realm of radiation detection and protection, holding promise for a wide array of applications in radiation-sensitive electronic systems.

Acknowledgement. This work was supported by the National Research Foundation of Ukraine, project 2020.02/0217 "Light-generation low-dimensional structures with polarized luminescence based on organic and inorganic materials."

REFERENCES

- [1] *Faiza Qammar M.* A Sequenced study of improved dielectric properties of carbon nanotubes and metal oxide-reinforced polymer composites / M. Faiza Qammar, S. U. Butt, Z. Malik, A.A. Alahamadi, A. Khattak // *Materials*. – 2022. – Vol. 15(13). – P. 4592.

- [2] *Khachatryan G.* Design of carbon nanocomposites based on sodium alginate/chitosan reinforced with graphene oxide and carbon nanotubes / G. Khachatryan, K. Khachatryan, J. Szczepankowska, M. Krzan, M. Krystyan // *Polymers*. – 2023. – Vol. 15(4). – P. 925.
- [3] *Kuang T.* Creating poly (lactic acid)/carbon nanotubes/carbon black nanocomposites with high electrical conductivity and good mechanical properties by constructing a segregated double network with a low content of hybrid nanofiller / T. Kuang, M. Zhang, F. Chen, Y. Fei, J. Yang, M. Zhong, ... T. Liu // *Advanced Composites and Hybrid Materials*. – 2023. – Vol. 6(1). – P. 48.
- [4] *Yang F.* Chirality pure carbon nanotubes: Growth, sorting, and characterization / F. Yang, M. Wang, D. Zhang, J. Yang, M. Zheng, Y. Li // *Chemical reviews*, 2020 120(5), 2693-2758.
- [5] *Civalek Ö.* Forced vibration analysis of composite beams reinforced by carbon nanotubes / Ö. Civalek, Ş. D. Akbaş, B. Akgöz, S. Dastjerdi // *Nanomaterials*. – 2023. – Vol. 11(3). – P. 571.
- [6] *Sambyal P.* Ultralight and mechanically robust Ti₃C₂T_x hybrid aerogel reinforced by carbon nanotubes for electromagnetic interference shielding / P. Sambyal, A. Iqbal, J. Hong, H. Kim, M. K. Kim, S. M. Hong, ... C. M. Koo // *ACS Applied Materials & Interfaces*. – 2019. – Vol. 11(41). – P. 38046-38054.
- [7] *Kumar A.* A review on the mechanical properties of polymer composites reinforced by carbon nanotubes and graphene / A. Kumar, K. Sharma, and A. R. Dixit // *Carbon Letters*. – 2021. – Vol. 31(2). – P. 149-165.
- [8] *Gilshateyn E. P.* Mechanically tunable single-walled carbon nanotube films as a universal material for transparent and stretchable electronics / E. P. Gilshateyn, S. A. Romanov, D. S. Kopylova, G. V. Savostyanov, A. S. Anisimov, O. E. Glukhova, A. G. Nasibulin // *ACS applied materials & interfaces*. – 2019. – Vol. 11(30). – P. 27327-27334.
- [9] *Chao M.* Functionalized multiwalled carbon nanotube-reinforced polyimide composite films with enhanced mechanical and thermal properties / M. Chao, Y. Li, G. Wu, Z. Zhou, L. Yan // *International Journal of Polymer Science*. – 2019. – P. 9302803.
- [10] *Lee Y. H.* Self-healing nanocomposites with carbon nanotube/graphene/Fe₃O₄ nanoparticle tricontinuous networks for electromagnetic radiation shielding / Y.H. Lee, L. Y. Wang, C. Y. Tsai, C. W. Lee // *ACS Applied Nano Materials*. – 2022. – Vol. 5(11). – P. 16423-16439.
- [11] *Sayyed M. I.* Radiation shielding properties of bi-ferroic ceramics added with CNTs / M. I. Sayyed, E. Hannachi, Y. Slimani, M. U. Khandaker, M. Elsafi // *Radiation Physics and Chemistry*. – 2022. – Vol. 200. – P. 110096.
- [12] *Heydari H. R.* Cell line selection through gamma irradiation combined with multi-walled carbon nanotubes elicitation enhanced phenolic compounds accumulation in *Salvia nemorosa* cell culture / H. R. Heydari, E. Chamani, B. / *Esmailpour Plant Cell, Tissue and Organ Culture (PCTOC)*. – 2020. – Vol. 142(2). – P. 353-367.
- [13] *Basgoz O.* Synthesis and structural, electrical, optical, and gamma-ray attenuation properties of ZnO-multi-walled carbon nanotubes (MWCNT) composite separately incorporated with CdO, TiO₂, and Fe₂O₃ / O. Basgoz, O. Guler, E. Evin, C. Yavuz, G. ALMisned, S. F. Issa, ... H.O. Tekin // *Ceramics International*. – 2022. – Vol. 48(11). – P. 16251-16262.

- [14] Karbovnyk I. Random nanostructured metallic films for environmental monitoring and optical sensing: experimental and computational studies / I. Karbovnyk, J. Collins, I. Bolesta, A. Stelmashchuk, Kolkevych A., S. Velupillai, H. Klym, O. Fedyshyn, S. Tymoshuk, I. Kolych // Nanoscale research letters. – 2015. – Vol. 10(1) . – P. 151.
- [15] Karbovnyk I. Effect of radiation on the electrical properties of PEDOT-based nanocomposites / I. Karbovnyk, I. Olenych, O. Aksimientyeva, H. Klym, O. Dzendzelyuk, O. Hrushetska // Nanoscale research letters. – 2016. – Vol. 11. – P. 1-5.

РАДІАЦІЙНО-ІНДУКОВАНІ ЗМІНИ ЕЛЕКТРИЧНИХ ВЛАСТИВОСТЕЙ PEDOT:PSS/CNT НАНОКОМПЗИТИВ

І.В. Жиденко^{1,2}, Г.І. Клим^{2,3}

¹Львівський державний університет безпеки життєдіяльності,

Вул. Клепарівська, 35, 79007, Львів, Україна

zhiddenkoillya@gmail.com, illia.v.zhydenko@lpnu.ua

²кафедра спеціалізованих комп'ютерних систем,

Національний університет «Львівська політехніка»,

вул. С. Бандери, 12, 79013 Львів, Україна

halyna.i.klym@lpnu.ua, klymha@yahoo.com

³кафедра радіоелектронних і комп'ютерних систем,

Львівський національний університет імені Івана Франка,

вул. Драгоманова, 50, 79005, Львів, Україна

halyna.klym@lnu.edu.ua

Досліджено вплив іонізуючого β - and γ -випромінювання на наносистеми PEDOT:PSS-CNT з використанням ізотопу ^{226}Ra з активністю 0,1 мКі. Показано, що неопромінений зразок має питомий опір вище 28 кОм у діапазоні частот від постійного струму до 100 кГц. Опір падає до 25 кОм, оскільки частота збільшується до 1 МГц. Після 30-хвилинного опромінення опір в низькочастотному діапазоні збільшується приблизно на 2 кОм, а ефект після 30 хвилин подвоюється.

Змодельовано загальний низькочастотний опір композиту PEDOT:PSS-CNT як паралельне з'єднання опору R_{poly} та опору, пов'язаного з нанотрубками R_{nt} , припускаючи, що нанотрубки створюють паралельний провідний шлях до того, що утворюється полімерною структурою. На основі отриманого значення загального низькочастотного опору з експерименту (4,7 кОм) та, виконуючи прості обчислення для двох паралельних резисторів, одержано значення 5,7 кОм для R_{nt} . Показано, що подальше збільшення нанотрбок у полімері приводить до зниження опору одержаних нанокмпозитів. Продемонстровано, що одночасний вплив β - та γ -випромінювання з джерела ^{226}Ra збільшує опір композиту PEDOT:PSS-CNT. Такі трансформації зумовлені одночасними змінами в R_{nt} та R_{poly} . Після поглинання початкової дози, загальний опір композиту R_{nt} буде незмінним (5,7 кОм), паралельно пов'язаним з підвищеним R_{poly} (30 кОм). В результаті був би одержаний загальний опір 4,8 кОм, що є нижче від експериментально спостережуваного значення (5 кОм). Тому необхідним є розгляд обидвох радіаційно-індукованих складових у R_{nt} та R_{poly} .

Одна з можливих причин збільшення R_{poly} може бути пов'язана з радіаційно стимульованими паралельними процесами руйнування і з'єднання у полімері. Розрив

ланцюга полімеру внаслідок поглинутого іонізуючого випромінювання призводить до перенесення заряду через π -електронні спряження, що супроводжується зменшенням електропровідності гібридної системи. Поява незавершених зв'язків з некомпенсованими валентними електронами дозволяє блокувати ланцюги і стимулює «зшивання» полімеру. Ці зміни є незворотними, а ступінь перетворень залежить від дози опромінення, а також від структури полімеру.

Для підтвердження експериментальних результатів було проведено чисельне моделювання. Полімерну матрицю, наповнену нанотрубками, було змодельовано як 3D паралелепіпед з «электродами», прикріпленими до її протилежних країв, випадково заповненими відкритими провідними «нанотрубками» циліндричної форми. Результати розрахунків дозволили візуалізувати об'ємний розподіл нанотрубок та виділити провідні доріжки. Обчислена мінімальна об'ємна частка нанотрубок, необхідна для того, щоб змодельований композит став електропровідним, відома як поріг перколяції, становила близько 1%, що нижче, ніж експериментально спостережуваний поріг. Різниця може бути обумовлена кількома факторами, включаючи приблизні моделі (обмежена кількість елементів у системі) або умови диспергування нанотрубок під час одержання зразків.

Ключові слова: нанокомпозит, нанотрубка, опромінення, полімерна матриця, електричні властивості, комп'ютерне моделювання.

Стаття надійшла до редакції 09.09.2023

Прийнята до друку 15.09.2023